

## RECOMBINATION EFFECTS ON SUPERNOVAE LIGHT-CURVES

TOMER GOLDFRIEND<sup>1,2</sup>, EHUD NAKAR<sup>2</sup> AND RE'EM SARI<sup>1</sup>  
*Draft version June 21, 2021*

### ABSTRACT

Supernovae of type IIP are marked by the long plateau seen in their optical light curves. The plateau is believed to be the result of a recombination wave that propagates through the outflowing massive hydrogen envelope. Here, we analytically investigate the transition from a fully ionized envelope to a partially recombined one and its effects on the SN light curve. The motivation is to establish the underlying processes which dominate the evolution at late times when recombination takes place in the envelope, yet early enough so that <sup>56</sup>Ni decay is a negligible source of energy. We assume a simple, yet adequate, hydrodynamic profile of the envelope and study the mechanisms which dominate the energy emission and the observed temperature. We consider the diffusion of photons through the envelope while analyzing the ionization fraction and the coupling between radiation and gas. We find that once recombination starts, the observed temperature decreases slowly in time. However, in a typical red supergiant (RSG) explosion, the recombination wave does not affect the bolometric luminosity immediately. Only at later times, the cooling wave may reach layers that are deep enough to affect the luminosity. We find that the plateau is not a generic result of a recombination process in expanding gas. Instead it depends on the density profile of the parts of the envelope which undergo recombination. Our results are useful to investigate the light curves of RSG explosions. We show the resulting light curves of two examples of RSG explosions according to our model and discuss their compatibility with observations. In addition, we improve the analytical relations between the plateau luminosity and plateau duration to the properties of the pre-explosion progenitor (Arnett 1980; Popov 1993).

### 1. INTRODUCTION

Type IIP supernova (SN) is the most common supernova type (Li et al. 2011). It is marked by H lines in its spectra and by a long,  $\approx 100$  days optical plateau that starts between a few days to a few weeks after the explosion. The progenitors of type IIP SNe are red supergiants (RSGs), which exhibit an extended H envelope (Smartt et al. 2004; Van Dyk et al. 2003; Maund & Smartt 2009). The initial temperature of the envelope as it starts to expand, after the shock crossing, is high ( $> 10^5$  K), but it drops with time due to adiabatic losses. The observed temperature drops rapidly until it reaches the H recombination temperature,  $\approx 7000$  K, where it remains rather constant during the entire plateau phase. For that reason it is believed that recombination is the source of the long lasting optical plateau.

The initial conditions for the beginning of the recombination phase are set by the radiation dominated shock that crosses the envelope and explodes the star. The shock accelerates in the decreasing density gradient near the edge of the stellar envelope and determines the velocity and internal energy profile of the envelope. Once the shock reaches to a point where the distance to the edge of the star is comparable to the shock's width, it "breaks out". This is the first electro-magnetic signal of a SN explosion (Colgate 1974; Falk 1978; Klein & Chevalier 1978; Imshennik et al. 1981). The envelope continues to accelerate while photons continuously diffuse out through

it (Matzner & McKee 1999). The acceleration ends before a considerable expansion takes place and at the end of this phase there is a hot, ionized, radiation dominated envelope in a homologous expansion. The internal regions are dense with large optical depth and they lose energy adiabatically. The external regions have a lower optical depth and photons can diffuse through them over a dynamical time. The expansion reduces the envelope optical depth, enabling photons to diffuse from deeper regions in the envelope. At breakout, the temperature of the external regions from where radiation can diffuse to the observer is  $\sim 30$  eV (Nakar & Sari 2010). It drops over a week or two until it reaches the recombination temperature. Until that time the entire envelope is ionized and its opacity is Thomson opacity. Once recombination starts in the outer layers it leads to a sharp drop in the opacity of these layers. The fast escape of radiation via the low opacity recombined regions causes a fast drop in the temperature also in the ionized regions which lies just behind the recombined layer. This cooling leads to farther recombination which in turn leads to drop in the opacity and so on. The resulting picture is a recombination wave, followed by cooling, which propagates inward (in Lagrangian sense) through the envelope. The propagation of this wave depends on the velocity and on the internal energy profiles of the envelope and obtaining an analytic understanding of this process is the goal of this paper.

In this work we derive an analytical model to study the effect of recombination on SNe light curves. We examine the problem of a homologous expanding envelope which cools adiabatically, together with energy transport by diffusion of photons. We assume that <sup>56</sup>Ni radioactive decay is a negligible source of energy. This

goldfriend@poat.tau.ac.il

<sup>1</sup>Racah Institute for Physics, The Hebrew University, Jerusalem, 91904, Israel

<sup>2</sup>The Raymond and Berverly Sackler School of Physics and Astronomy, Tel Aviv University, 69978 Tel Aviv, Israel

condition holds for a typical explosion of an RSG, in which the radioactive decay luminosity is low compared to the release of the thermal energy deposited by the shock (see discussion in appendix C). In addition, we neglect the effect of radioactive decay on the opacity, due to non-thermal photoionization. Our model is based on recent work by Nakar & Sari (2010) (NS10 hereafter) where early light curves, before recombination has a significant role, were derived. As a result, we can draw the evolution of the light curves from the initial pulse (shock breakout) up to the time when most of the envelope is recombined. We find that it is essential to take into account the coupling between matter and radiation since in the recombined gas the opacity can vary by orders of magnitude while the temperature changes only by a factor of two. For that reason it is essential to find the exact temperature in this layer and thus the opacity drop. Here, the radiation-gas coupling plays the main role since a drop in the temperature reduces the coupling (along with the opacity), while in order for the temperature to drop a minimal coupling is required. This feedback of the coupling on the temperature is what sets the exact temperature and opacity drop in the recombined layer. By solving self consistently for the radiation-gas coupling and the opacity drop, within the expanding gas velocity and internal energy profiles, we find a solution for the propagation of the recombination wave and for the resulting observed radiation.

The propagation of a recombination wave in SNe envelope was studied analytically in previous works (Grassberg et al. 1971; Grassberg & Nadyozhin 1976; Popov 1993; Rabinak & Waxman 2011). However, these works used more limited assumptions compared to our model, such as full coupling between gas and radiation. In addition, some of these models were derived for physical conditions which are not applicable for SNe envelope, such as homogeneous envelope (Popov 1993). A comparison to these previous works is discussed in section 7. We also compare qualitatively between our results and the results from recent numerical works, such as Utrobin (2007); Kasen & Woosley (2009) and Bersten et al. (2011), which examined the light curves of type IIPs and discussed in detail the properties of the recombination wave in the envelope.

The paper is organized as follows. In section 2 we introduce the hydrodynamical profile of the envelope we use in our model. In section 3 we discuss the evolution at early stages, up to the onset of recombination, according to NS10. Then, in section 4 we describe how recombination, through the decrease in the ionization fraction, affects the diffusion of energy and production of new photons in the envelope. In section 5 we introduce the solution to these equations and calculate the luminosity and the observed temperature for a given hydrodynamical profile of the envelope. We treat separately two different cases. The first is the realistic case where the ionization fraction is parametrized as a continuous function of the temperature (§5.1). The second is the academic, yet enlightening, case where opacity is parametrized by a step function of the temperature (appendix A). In section 6 we apply the results of §5.1 and appendix A to an analytic description of a typical RSG expanding envelope. In addition, we apply the model to profiles given numerically from a simulation of RSG explosion and derive the

corresponding light curves semi-analytically. In section 7 we compare results from previous analytical and numerical works to our results. Finally in 8 we summarize our findings.

## 2. THE HYDRODYNAMIC PROFILE OF THE ENVELOPE

The expanding envelope can be considered as a series of successive shells (NS10). For each shell, there are no considerable changes in the hydrodynamical parameters over the shell width. Following the breakout, the evolution of each shell can be divided into two phases: planar phase, before the shell radius doubles, and spherical phase at later times. Since we are interested in later times we discuss only the spherical phase of the shells which takes place after acceleration ends and the envelope expansion is homologous. We treat the density and adiabatic energy profiles of the envelope during the spherical phase as given. We parametrize these profiles by power laws. The applicability of such parametrization for SNe envelope is discussed below.

The evolution of the density is given by

$$\rho(r, t) = f_\rho r^{-k} t^{k-3}, \quad (1)$$

where  $k$  is a positive constant and  $f_\rho$  is a constant which depends on the initial properties of the progenitor. Each mass shell is characterized by its mass,  $m$ . During the spherical phase, the width of each shell is comparable to the radius of the shell  $r \approx v(m)t$ , thus, equation (1) corresponds to the velocity profile

$$v(m) \propto m^{-\frac{1}{k-3}}. \quad (2)$$

At a given time we parametrize the internal energy in the regions that cools adiabatically as

$$E_{\text{ad}}(m, t) = f_{\text{ad}} m^s r^{-1}, \quad (3)$$

where  $s$  is a positive constant and  $f_{\text{ad}}$  depends on the initial conditions of the progenitor and the explosion.  $E_{\text{ad}}$  depends on  $t$  through  $r = v(m)t$ .

Equation (2) shows that the parameter  $k$  is related to the coasting velocity profile of the envelope. In order to determine the parameter  $s$ , additional information about the profiles of the velocity and density right after the passage of the shock,  $v_i(m)$  and  $\rho_i(m)$ , is needed. This is because the initial thermal energy of each shell following the breakout is  $\sim mv_i^2$ , so  $E_{\text{ad}}(m, t) = mv_i^2(\rho/\rho_i)^{1/3} = mv_i^2(m/\rho_i)^{1/3}r^{-1}$ .

The power laws parametrization is applicable at the external part of the SN envelope, located internal to the point from which the shock breaks out ( $\sim 10\%$  of the envelope mass). This part controls the light curves at early stages. The profiles in these external parts can be approximated analytically with  $k = 9.5 - 12$  and  $s = 0.8 - 0.9$  (Matzner & McKee 1999, and references therein). At late stages of the evolution, deeper shells become transparent and control the light curve. These shells are characterized with softer density profiles, and a description of the evolution using power-laws is less accurate.

In sections 3 and 5 we provide a general solution for single power law profiles described by the parameters  $k$  and  $s$ . For simplicity, together with the general solution, we introduce our results for specific values of  $k$  and  $s$ . For the outer layers (section 3) we use  $k = 12$  and  $s = 0.9$ .

For inner parts, where recombination takes place (section 5), we take representative values that are deduced from a numerical simulation. The basic equations of our model (introduced in §4.2), which govern the evolution, can be solved numerically for any given profiles of the envelope. Example of a numerical solution is given in §6.2.

### 3. EARLY LIGHT-CURVES

#### 3.1. Luminosity Shell and Color Shell

While the envelope is highly ionized and all the relevant shells are at their spherical phase, the optical depth and the diffusion time of each shell are

$$\tau \approx \kappa_T \rho r \quad , \quad t_d \approx \frac{\tau r}{c}, \quad (4)$$

where  $\kappa_T$  is Thomson opacity for ionized gas and  $c$  is the speed of light. The luminosity is dictated by the luminosity shell from which photons diffuse out effectively. In this shell the diffusion time is equal to the time since explosion, which is also the dynamical time of the shell- $r/v(m)$ . Photons in shells internal to the luminosity shell can barely escape because the diffusion time there is longer. On the other hand, shells external to the luminosity shell have already released their energy at earlier times. At any given time we can find the mass of the luminosity shell by requiring

$$\tau(\hat{m}, t) = c/v(\hat{m}). \quad (5)$$

The properties of the luminosity shell are marked with superscript  $\hat{\phantom{x}}$ . Here we repeat the analysis of NS10 in terms of the parameters  $k$  and  $s$ . Using equations (2), (3) and (4), and the definition of the luminosity shell (5), we find

$$\hat{m}(t) \propto t^{\frac{2(k-3)}{k-2}} \approx t^{1.8},$$

$$L(t) = \hat{E}_{\text{ad}}/t \propto t^{-\frac{2(1-s)(k-3)}{k-2}} \approx t^{-0.17}. \quad (6)$$

In this section we use  $k = 12$  and  $s = 0.9$  as canonical values.

The energy density in shells internal to the luminosity shell is dominated by adiabatic cooling (equation (3)). At any given time the luminosity through shells external to the luminosity shell is constant and given by equation (6). The energy density,  $\epsilon$ , in these shells is determined by the diffusion of total luminosity  $L$  with a diffusion time  $t_d$  given in equation (4),

$$\epsilon(m, t) = \begin{cases} \frac{E_{\text{ad}}}{r^3} & m > \hat{m} \\ \frac{L\tau}{cr^2} & m < \hat{m} \end{cases}. \quad (7)$$

Note that the above expression holds up to the shell in which  $\tau \approx 1$ .

When the radiation is thermalized, the temperature is a blackbody temperature given by

$$T_{\text{BB}} = (\epsilon/a)^{1/4}. \quad (8)$$

Where  $a$  is the radiation constant. The optical depth of the luminosity shell is always greater than 1. Thus, photons which escape from the luminosity shell can have many interactions with the gas as they are traveling through the envelope until they finally leave it at the point where the optical depth is  $\sim 1$ . For the relevant physical conditions the luminosity shell is in thermal

equilibrium ( $\hat{T} = \hat{T}_{\text{BB}}$ ), see §3.2.

Consider shells at the region external to the luminosity shell -  $r > \hat{r}$ . The photons dominate the heat capacity, hence, the total radiation flux in this region is independent of the coupling between the photons and the gas. As long as the radiation is in thermal equilibrium, the photon number flux increases with  $r$  and the typical energy of each photon, which originated in the luminosity shell, is changed while it travels outward. Thus, in order to keep the radiation thermalized, electrons in each shell must generate sufficient amount of new photons which share their energy with photons which arrive from internal shells. External to the point in which the radiation departs from thermal equilibrium, the photon number flux is fixed (at a given time) and the temperature can not change. Hence, the observed temperature is the blackbody temperature of the outermost shell which is in thermal equilibrium.

We assume that free-free emission is the dominant process for photons production. Similarly to NS10 we define a thermal coupling coefficient

$$\eta \equiv \frac{n_{\text{BB}}}{t_d \cdot \dot{n}_{\text{ph,ff}}(T_{\text{BB}})}, \quad (9)$$

where  $n_{\text{BB}} = aT_{\text{BB}}^3/3k_B$  is the density of photons with  $h\nu \approx 3k_B T_{\text{BB}}$  and  $\dot{n}_{\text{ph,ff}}(T) = 3.5 \times 10^{36} \text{ s}^{-1} \text{ cm}^{-3} \rho^2 T^{-1/2}$  is the free-free emission rate, per unit volume, of photons with energy  $h\nu \approx 3k_B T$ . The parameter  $\eta$  defined this way, is the time required to achieve thermal equilibrium ignoring photon diffusion  $\sim n_{\text{BB}}/\dot{n}_{\text{ph,ff}}(T_{\text{BB}})$ , divided by the diffusion time. Photons released from the luminosity shell ( $\hat{\eta} < 1$ ) change their typical energy up to the shell in which  $\eta = 1$ , where the observed temperature is determined. Thus, the observed spectrum is blackbody at a temperature of that shell, which we call the ‘‘color’’ shell. We denote the properties of the color shell with the subscript  $\text{cl}$ . The evolution of the color temperature and the color shell mass are given by

$$T_{\text{cl}}(t) \propto t^{\frac{2(k-3)(6ks-11k-4s+14)}{(k-2)(17k-23)}} \approx t^{-0.56},$$

$$m_{\text{cl}}(t) \propto t^{-\frac{14(-ks-k+3s+1)(k-3)}{(k-2)(17k-23)}} \approx t^{1.33}, \quad (10)$$

where the color shell is defined by  $\eta(m_{\text{cl}}, t) = 1$ . The gas and radiation must have one temperature up to the color shell, but outward of the color shell they can decouple, where the radiation temperature is constant while the gas temperature may drop. The complete equations of the color shell evolution are (4), (6), (19) and (21) in NS10. The pre-factors are related to the initial conditions of the progenitor. For further discussion on the coupling between radiation and matter in ionized medium see NS10.

#### 3.2. Initial conditions for recombination

We summarize the state of the envelope just before recombination starts. That is, we draw the initial conditions for the problem we solve in the next sections. We assume that just before recombination starts the envelope is in its spherical phase, i.e. all the shells which dominate the light curves are in their spherical phase. In addition, we assume that the luminosity shell is already in thermal equilibrium ( $\hat{\eta} < 1$ ) so the color shell

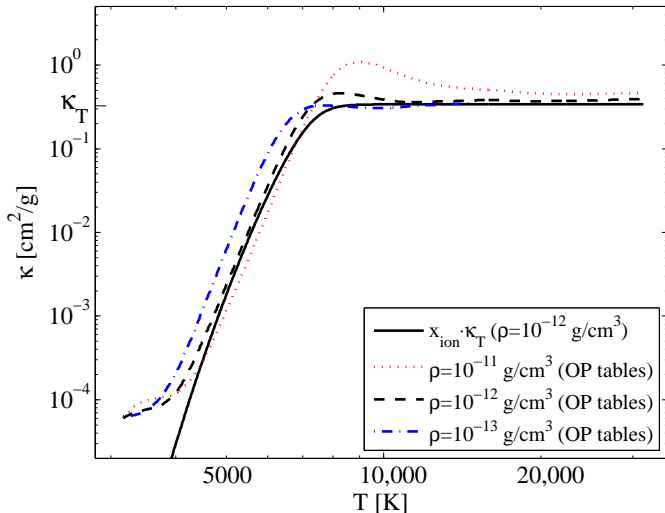


**Figure 1.** Rosseland opacity using OP tables (Seaton 2005) and Saha equation. The dash-dotted lines are Rosseland opacities for  $Y=0.3, Z=0.02$  (solar metallicity) taken from the tables. The solid line is a theoretical line  $\kappa = x_{\text{ion}}\kappa_T$  where  $x_{\text{ion}}$  is the ionization fraction given by Saha equation.

is located external to the luminosity shell. These physical conditions are adequate for an explosion of a RSG (NS10).

Before recombination starts the evolution of the luminosity shell and the luminosity are given in equation (6). The recombination temperature,  $T_{\text{rec}}$ , is defined as the temperature in which there is a sharp change in the opacity (figure 1). When the color temperature drops below the recombination temperature we must take into account the effect of recombination. We define the recombination time,  $t_{\text{rec}}$ , by  $T_{\text{cl}}(t_{\text{rec}}) = T_{\text{rec}}$ . In the next section we find the evolution of the luminosity shell and the color shell after the onset of recombination. The solution is written as a function of the conditions when recombination starts:  $\hat{m}(t_{\text{rec}})$ ,  $m_{\text{cl}}(t_{\text{rec}})$ ,  $L(t_{\text{rec}})$  and  $T_{\text{cl}}(t_{\text{rec}}) = T_{\text{rec}}$ .

#### 4. THE EFFECT OF RECOMBINATION

##### 4.1. Modeling the Opacity and the Free-Free Process

Recombination changes the opacity and the rate of generation of new photons. In section 3, considering the evolution before recombination starts, we take these quantities to be  $\kappa = \kappa_T$  and  $\dot{n}_{\text{ph}} = \dot{n}_{\text{ph,ff}} = 3.5 \times 10^{36} \rho^2 T^{-0.5}$  respectively. In our model, we assume that when recombination occurs, electron scattering still dominates the opacity and that free-free emission still dominates the photon production rate<sup>3</sup>. Thus, we write  $\kappa = x_{\text{ion}} \cdot \kappa_T$  and  $\dot{n}_{\text{ph}} = x_{\text{ion}}^2 \dot{n}_{\text{ph,ff}}$ , where  $x_{\text{ion}}$  is the ionization fraction. These two quantities decrease as electrons and ions become less abundant. Figure 1 shows that for the low densities ( $\leq 10^{-12} \text{ g cm}^{-3}$ ) and temperatures between 3000 K to 12,000 K, indeed Thomson scattering provides almost all the opacity. This range of densities is the one found in RSG explosions at  $t_{\text{rec}}$ . A good approximation for the ionization fraction can be obtained from the

<sup>3</sup> Even in the case that bound-free is the dominant process, which might be the case when recombination occurs, the expression for the production rate differs from that of the free-free process only by a constant that depends (linearly) on the metallicity.

Saha equation. However, to obtain analytical results, we parametrize the ionization fraction as

$$x_{\text{ion}} = \begin{cases} 1 & T > T_{\text{rec}} \\ (T/T_{\text{rec}})^{11} & T < T_{\text{rec}} \end{cases} \quad (11)$$

In addition, in appendix A we derive an analytical solution for the parametrization of the ionization fraction as a step function, equation (A1).

We neglect the effects of velocity gradients on opacity through atomic line broadening and the increase of ionization ratio by non-thermal  $\gamma$  rays from  $^{56}\text{Ni}$  radioactive decay (see discussion in section 8). We also neglect the energy released by recombination (see section 7).

##### 4.2. Basic Equations

Recombination starts to affect the evolution when the color temperature equals the recombination temperature. Let us consider the envelope from the luminosity shell out to the point where  $T = T_{\text{rec}}$ . The energy density of this part of the envelope is dictated by the diffusion of photons (equation (7)). At the point where  $T = T_{\text{rec}}$  the opacity drops and photons escape “more easily” causing a sharp decrease in the energy density. This drop is related to a drop in the temperature which in turn decreases the opacity. Therefore, from  $t = t_{\text{rec}}$  recombination moves inward (in the Lagrangian sense) and starts to reach deeper shells. We call the shell in which  $T = T_{\text{rec}}$  the *recombination shell*, and denote its properties by the subscript  $\text{rec}$ . Because the change in the opacity at  $T_{\text{rec}}$  is sharp enough, the energy density and the optical depth profiles changes significantly within this shell. While these profiles inside the recombination shell are complicated (see, for example figure 2), the properties of shells located far from the recombination shell (in or out) can be easily determined. This is because within those shells all the hydrodynamical parameters can be approximated as homogeneous. The optical depth and thermal coupling coefficient of such shells are given by

$$\tau(m \neq m_{\text{rec}}) = \frac{c}{\hat{v}(t_{\text{rec}})} \left( \frac{\rho}{\hat{\rho}(t_{\text{rec}})} \right) \left( \frac{r}{\hat{r}(t_{\text{rec}})} \right) x_{\text{ion}}(T), \quad (12)$$

$$\eta(m \neq m_{\text{rec}}) = \left( \frac{T_{\text{BB}}}{T_{\text{rec}}} \right)^{\frac{7}{2}} \left( \frac{\rho}{\rho_{\text{cl}}(t_{\text{rec}})} \right)^{-3} \times \left( \frac{r}{r_{\text{cl}}(t_{\text{rec}})} \right)^{-2} x_{\text{ion}}(T)^{-3}. \quad (13)$$

It is only the region between the luminosity shell and the color shell,  $\hat{r} \leq r \leq r_{\text{cl}}$ , which is relevant in order to understand the evolution, since beyond these two regions both the luminosity and the temperature are constant. Now, if the dependence of the opacity on temperature is strong enough, the color shell and recombination shell are the same, i.e.,  $r_{\text{rec}} \cong r_{\text{cl}}$ , at any time after  $t_{\text{rec}}$ . One can see that by assuming the contrary, that  $r_{\text{rec}} \ll r_{\text{cl}}$ , then equations (7)-(8) imply that the temperature is an increasing function of radius ( $T \propto (r/\rho)^{1/7}$  for  $x_{\text{ion}} \propto T^{11}$ ), which is not physical. Therefore, within the recombination shell the temperature drops sharply and by the end of the shell the system must leave thermal equilibrium with  $\eta = 1$ . The radiation temperature is then fixed external of this point, and is not an increas-

ing function of  $r$ . This shows that recombination and thermal coupling are intimately related and there could be no correct treatment of recombinations that ignores thermal coupling.

While the recombination wave is described by the non uniform temperature profile in the recombination shell, we find the dynamics of the recombination shell without dealing with the profiles inside it. Instead we consider the properties on its boundaries, where all the properties -  $\epsilon$ ,  $T_{\text{BB}}$ ,  $x_{\text{ion}}$ ,  $\tau$  and  $\eta$ , are approximately homogeneous and given by equations (7), (8), (11), (12) and (13). We indicate the properties of the internal and external boundary with the sub-scripts  $_{\text{rec-in}}$  and  $_{\text{rec-out}}$ . The internal boundary is located at a distance  $\sim r_{\text{rec}}$  inward from the point where  $T = T_{\text{rec}}$  and the external boundary, which coincides with the color shell, at a distance  $\sim r_{\text{rec}}$  outward from that point. The density of the recombination shell is roughly uniform (does not change on scale much smaller than  $r$  like the temperature or energy density) and is given by  $\rho_{\text{rec}} \sim m_{\text{rec}}/(v(m_{\text{rec}})t)^3$ .

The internal boundary of the recombination shell is not affected by recombination. The value of  $\epsilon_{\text{rec-in}}$  and  $\eta_{\text{rec-in}}$  can be approximated by equations (7)-(8) and (12)-(13) with  $m = m_{\text{rec}}$  and  $x_{\text{ion}} = 1$ . This implies that  $\eta_{\text{rec-in}} < 1$  and  $\epsilon_{\text{rec-in}} > aT_{\text{rec}}^4$ . The properties of the external boundary are dictated by the end of thermal coupling -  $\eta = 1$ . The luminosity in the recombination shell is dictated by the inner region: the luminosity shell when  $\hat{m} > m_{\text{rec}}$  and the inner boundary of the recombination shell itself otherwise<sup>4</sup>. A schematic description of the energy density profile within the recombination shell is given in figure 2.

To summarize, for  $t \geq t_{\text{rec}}$ , the equations governing the dynamics of the three characteristic shells are

$$\begin{cases} \tau(\hat{m}) = c/v(\hat{m}) & , \text{ if } \hat{m} > m_{\text{rec}} \\ \hat{m} = m_{\text{rec}} & , \text{ otherwise} \end{cases}, \quad (14a)$$

$$L = \frac{E_{\text{ad}}(\hat{m})}{t} = \frac{aT_{\text{cl}}^4 c r_{\text{rec}}}{x_{\text{ion}}(T_{\text{cl}})\kappa T \rho_{\text{rec}}}, \quad (14b)$$

$$\eta_{\text{rec-out}} = 1. \quad (14c)$$

## 5. BOLOMETRIC LUMINOSITY AND OBSERVED TEMPERATURE

We now find the dynamics of the recombination shell and the evolution of the bolometric luminosity and color temperature. Here we use an approximate continuous function of the ionization fraction (equation 11), which closely follows the Saha equation (figure 1). In appendix A we solve the evolution when the ionization fraction is approximated by a step function (equation A1). A short summary of the main results in this case is presented in §5.2. The step function model is not realistic and is presented for deductive purposes and in order to allow a comparison of our analysis to an earlier model by Popov (1993), see section 7.

We introduce the results in a general form as a function of  $k$  and  $s$ . In addition, we provide the typical behavior

<sup>4</sup> The situation in which  $\hat{m} < m_{\text{rec}}$  is not relevant in our model. The dynamics of  $m_{\text{rec}}$  in this case, which is given solely by its adiabatic cooling (equation (3)), is inconsistent.

for  $k = 6$  and  $s = 0.95$ , which are found to be representative based on the numerical simulation presented in the next section. The solution is written as a function of the state of the envelope just before recombination. We denote the ratio between the luminosity and color shell masses at the beginning of recombination by

$$\Delta \equiv \left( \frac{m_{\text{cl}}(t_{\text{rec}})}{\hat{m}(t_{\text{rec}})} \right) < 1.$$

### 5.1. Ionization Fraction as a Continuous Function of $T$

Since  $x_{\text{ion}}$  is a continuous function of the temperature, the evolution is continuous (in contrast with the step function model discussed in the next subsection). As  $m_{\text{rec}}(t_{\text{rec}}) < \hat{m}(t_{\text{rec}})$  the bolometric luminosity is not affected by recombination when it starts. Only later, when the recombination wave arrives at the luminosity shell (so  $m_{\text{rec}} = \hat{m} = m_{\text{cl}}$ ) the recombination wave determines the luminosity. We denote that time as  $t_L$ .

The recombination shell is found by solving equations (14) for  $m_{\text{rec}}$  and  $T_{\text{cl}}$ . The expression for  $\eta_{\text{rec-out}}$  is approximated with equation (13) using  $m = m_{\text{rec}}$ ,

$$\eta_{\text{rec-out}} = \left( \frac{T_{\text{cl}}}{T_{\text{rec}}} \right)^{\frac{7}{2}} \left( \frac{\rho_{\text{rec}}}{\rho_{\text{cl}}(t_{\text{rec}})} \right)^{-3} \times \left( \frac{r_{\text{rec}}}{r_{\text{cl}}(t_{\text{rec}})} \right)^{-2} x_{\text{ion}}(T_{\text{cl}})^{-3}.$$

We find

$$m_{\text{rec}}(t) = m_{\text{cl}}(t) = \begin{cases} m_{\text{cl}}(t_{\text{rec}}) \left( \frac{t}{t_{\text{rec}}} \right)^{\frac{2(k-3)(-59ks+128k+177s-315)}{(k-2)(17k+87)}} & , t_{\text{rec}} \leq t \leq t_L \\ m_{\text{rec}}(t_L) \left( \frac{t}{t_L} \right)^{\frac{256(k-3)}{59ks+17k-177s+146}} & , t \geq t_L \end{cases} \quad (15)$$

$$\propto \begin{cases} t^{2.26} & , t_{\text{rec}} \leq t \leq t_L \\ t^{1.84} & , t \geq t_L \end{cases}.$$

Initially  $m_{\text{rec}}(t_{\text{rec}}) < \hat{m}(t_{\text{rec}})$  and we can see that indeed the recombination wave is moving inward (in the Lagrangian sense) faster than the ionized luminosity shell (equation 6). It reaches the luminosity shell at

$$t_L = \Delta^{-\frac{(k-2)(17k+87)}{2(-59ks+111k+177s-402)(k-3)}} t_{\text{rec}} \approx \Delta^{-1.31} t_{\text{rec}}. \quad (16)$$

At  $t \geq t_L$  recombination takes place within the luminosity shell and determines its location, so  $\hat{m} = m_{\text{rec}}$ . The color temperature is given by

$$T_{\text{cl}}(t) = \begin{cases} T_{\text{rec}} \left( \frac{t}{t_{\text{rec}}} \right)^{-\frac{2(k-3)(-6ks+11k+4s-14)}{(k-2)(17k+87)}} & , t_{\text{rec}} \leq t \leq t_L \\ T_{\text{cl}}(t_L) \left( \frac{t}{t_L} \right)^{-\frac{2(-7ks+11k+21s-26)}{59ks+17k-177s+146}} & , t \geq t_L \end{cases} \quad (17)$$

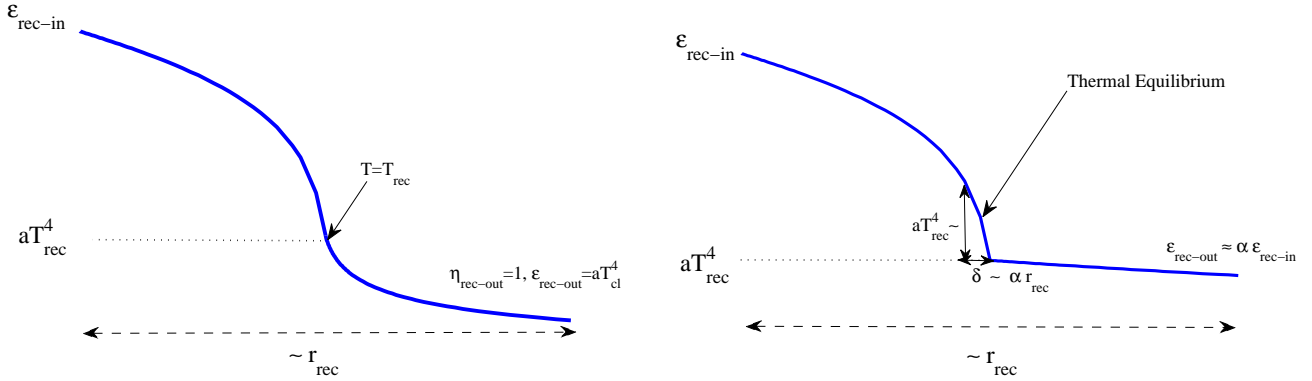


**Figure 2.** Schematic description of the energy density profile (logarithmic scale) inside the recombination shell when  $m_{\text{rec}} < \hat{m}$  for the two models-  $x_{\text{ion}} \propto T^{11}$  (**left**) according to §5.1 and  $x_{\text{ion}}$  is a step function (**right**) according to appendix A. The internal part is in thermal equilibrium and its temperature  $> T_{\text{rec}}$ . The luminosity is dictated by an inner shell. At the point where  $T = T_{\text{rec}}$  there is a sharp drop in the energy density because of the sharp decrease in the opacity at the external region. In both cases the point where  $T = T_{\text{rec}}$  is in thermal equilibrium. **In the left panel:** The temperature starts to flatten from the point where  $T = T_{\text{rec}}$  outward. The outer boundary is the outermost point which is in thermal equilibrium. **In the right panel:** The region in front of the point with  $T = T_{\text{rec}}$  is not necessarily in thermal equilibrium, see A.2 in appendix A. Behind the point with  $T = T_{\text{rec}}$  on a scale of  $\delta \sim \alpha r_{\text{rec}}$  the energy density is approximately  $aT_{\text{rec}}^4$ .

$$\propto \begin{cases} \propto t^{-0.17} & , t_{\text{rec}} \leq t \leq t_L \\ \propto t^{-0.1} & , t \geq t_L \end{cases} .$$

We can see that once recombination starts the temperature evolves much more slowly compared to its earlier evolution (equation 10), and it evolves even slower at  $t > t_L$ .

Finally, the bolometric luminosity, defined by equation (14b) is

$$L(t) = \begin{cases} L(t_{\text{rec}}) \left( \frac{t}{t_{\text{rec}}} \right)^{-\frac{2(1-s)(k-3)}{k-2}} & , t_{\text{rec}} \leq t \leq t_L \\ L(t_L) \left( \frac{t}{t_L} \right)^{\frac{2(69ks-17k-207s-18)}{59ks+17k-177s+146}} & , t \geq t_L \end{cases} \quad (18)$$

$$\propto \begin{cases} \propto t^{-0.07} & , t_{\text{rec}} \leq t \leq t_L \\ \propto t^{0.37} & , t \geq t_L \end{cases} .$$

At early times, when  $t < t_L$  and  $\hat{m} > m_{\text{rec}}$ , the luminosity does not depend on the dynamics of the recombination shell. The increase in the luminosity for  $t > t_L$  derived above could be expected as recombination exposes more internal shells. Examples for the above results are shown in figures 3 and 4, where they are compared to the results regarding the step function model.

### 5.2. Ionization Fraction as a Step Function

Here we summarize the main results obtained when the ionization fraction is approximated by a step function. The detailed analysis is presented in appendix A. As we argue below, this approximation is not physical. However, it emphasizes the importance of modeling the ionization fraction as a function which depends on the temperature when  $T < T_{\text{rec}}$  and it underlines some of

the ideas behind the way we analyze the recombination shell. In addition it can be compared with previous models which approximate the ionization fraction as a step function (Popov 1993; Grassberg & Nadyozhin 1976).

The strength of the discontinuity in the ionization fraction is given by the parameter  $\alpha$  in equation (A1). Just before recombination started the color shell has the properties-  $T_{\text{BB}}(m_{\text{cl}}(t_{\text{rec}}), t_{\text{rec}}) = T_{\text{rec}}$ ,  $\eta(m_{\text{cl}}(t_{\text{rec}}), t_{\text{rec}}) = 1$  and it is also the recombination shell. Because of the immediate change and the discontinuity in the opacity, at the onset of recombination  $m_{\text{rec}}$  is discontinuous. In addition, because of the immediate drop in the free-free emission rate, the mass of

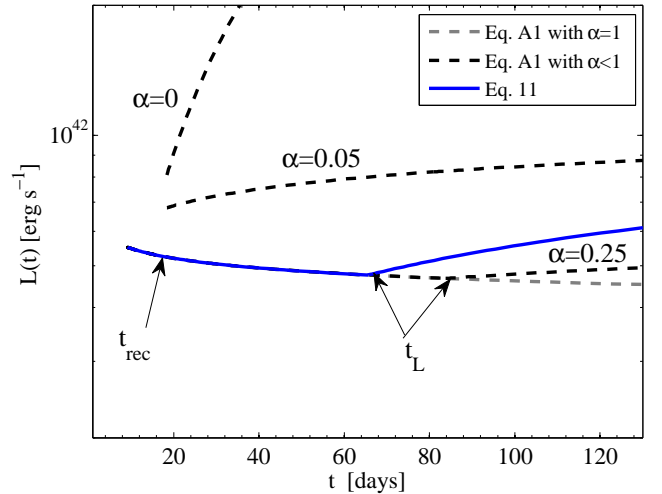


**Figure 3.** The bolometric luminosity for different approximations of the ionization fraction. The properties at  $t_{\text{rec}}$  are for a standard RSG progenitor ( $M_* = 15M_{\odot}$ ,  $R_* = 500R_{\odot}$ ) and explosion energy of  $10^{51}$  erg. After  $t_{\text{rec}}$  the hydrodynamic profile is approximated by  $k = 0.6$  and  $s = 0.95$ . The blue solid line is for ionization model  $x_{\text{ion}} \propto T^{11}$ . The black dashed lines are solutions for the step function models and the grey dashed line is for  $\alpha = 1$  where recombination has no effect.

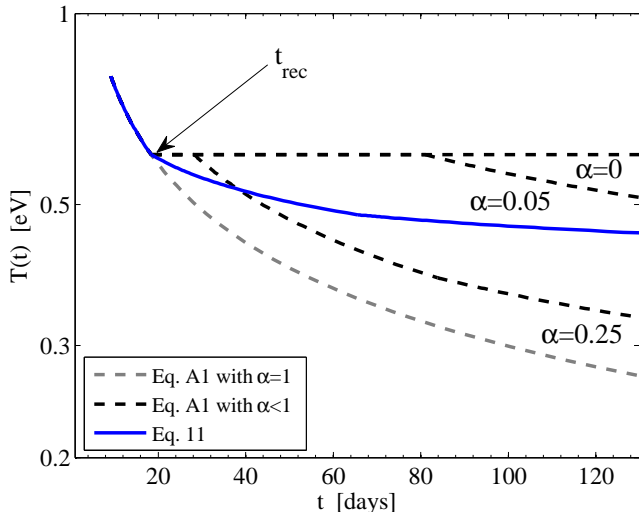


**Figure 4.** The observed temperature for different models. The initial conditions, hydrodynamic approximation and notations are the same as in figure 3. For the step function model, as the value of  $\alpha$  is smaller the observed temperature remains  $T_{\text{rec}}$  for longer times.

the color shell is also discontinuous. We find that from  $t = t_{\text{rec}}$  there is a transition time in which the recombination shell is also the color shell, but  $\eta_{\text{rec-out}} > 1$ . Once  $\eta_{\text{rec-out}} = 1$ , the color shell moves outward from the recombination shell. Hence, equations (14) are not relevant to the step function model and a more subtle analysis of the recombination shell profile is needed.

There is a diversity of types of evolution which depend on the value of  $\alpha$  with respect to  $\Delta$ . For example, we find a critical value  $\alpha_L$  such that for  $\alpha < \alpha_L$  there is a discontinuity in the luminosity at the onset of recombination. That is, when recombination starts it propagates on a very short time scale (shorter than the dynamical time) through the luminosity shell, exposing to the observer new regions. If  $\alpha = 0$ , this discontinuity is followed by a significant increase in the luminosity. There is also a range of values of  $\alpha$  which results in a short period of time where  $m_{\text{cl}} < m_{\text{rec}} < \hat{m}$  so the propagation of the recombination shell does not affect the luminosity nor the observed temperature.

For  $\alpha \ll 1$  there is a sharp increase in the luminosity when recombination starts, see figure 3. This does not agree with observations of SNe. On the other hand, for  $\alpha$  that is not much smaller than 1, the temperature drops below  $T_{\text{rec}}$  short time after recombination starts, see figure 4. The ionization fraction remains constant (since  $\alpha$  is constant) and therefore the physical conditions are not consistent, see figure 1.

## 6. APPLYING THE MODEL FOR A TYPICAL RSG PROGENITOR

### 6.1. General Properties of the Evolution

We apply the analytical model introduced above to a general explosion. We use the parameters  $k = 6$  and  $s = 0.95$  for the profiles of the envelope, (see equations 2 and 3). The results are written as a function of the properties of the pre-SN and the value of the recombination temperature. According to the early evolution, see

section 3, we find for the onset of recombination-

$$t_{\text{rec}} \approx 18 \text{ days } M_{15}^{-0.78} R_{500}^{0.98} E_{51}^{0.51} T_{\text{rec},0.6}^{-2.43}, \quad (19)$$

$$\Delta \equiv \left( \frac{m_{\text{cl}}(t_{\text{rec}})}{\hat{m}(t_{\text{rec}})} \right) \approx 0.38 M_{15}^{0.05} R_{500}^{-0.18} E_{51}^{0.19} T_{\text{rec},0.6}^{1.11}, \quad (20)$$

where,  $M_{15}$  is the initial mass of the progenitor in  $15M_{\odot}$  units,  $R_{500}$  is its initial radius in  $500R_{\odot}$  units,  $E_{51}$  is the explosion energy in  $10^{51}$  erg units and  $T_{\text{rec},0.6}$  is the recombination temperature in 0.6 eV units. We present here only results for the continuous ionization model (with  $x_{\text{ion}} \propto T^{11}$ ). Results for the step function model are presented in appendix A.

Using the results in §5.1 we find

$$t_L \approx 65 \text{ days } M_{15}^{-0.85} R_{500}^{1.23} E_{51}^{0.26} T_{\text{rec},0.6}^{-3.9}. \quad (21)$$

The bolometric luminosity is affected by recombination only after  $t_L$  and is given by

$$L(t) = \begin{cases} 6.5 \times 10^{41} \text{ erg s}^{-1} M_{15}^{-0.94} R_{500}^{0.98} E_{51}^{0.07} t_{\text{days}}^{-0.07} & t_{\text{rec}} < t < t_L \\ 10^{41} \text{ erg s}^{-1} M_{15}^{-0.57} R_{500}^{0.45} E_{51}^{0.86} T_{\text{rec},0.6}^{1.73} t_{\text{days}}^{0.37} & t > t_L \end{cases} \quad (22)$$

On the other hand, the observed temperature changes its evolution with time from  $t_{\text{rec}}$ ,

$$T_{\text{cl}}(t) = \begin{cases} 0.98 \text{ eV } M_{15}^{-0.13} R_{500}^{0.17} E_{51}^{0.09} T_{\text{rec},0.6}^{0.58} t_{\text{days}}^{-0.17} & t_{\text{rec}} < t < t_L \\ 0.72 \text{ eV } M_{15}^{-0.07} R_{500}^{0.08} E_{51}^{0.07} T_{\text{rec},0.6}^{0.87} t_{\text{days}}^{-0.1} & t > t_L \end{cases} \quad (23)$$

The observed temperature is  $T_{\text{rec}} \approx 0.6$  eV at  $t_{\text{rec}}$  by definition, then it drops to  $\Delta^{0.22} T_{\text{rec}} \approx 0.5$  eV at  $t_L$ . For  $t > t_L$  it is almost constant with time.

### 6.2. Numerical and Analytical Examples

We use our model to draw the light curves for an explosion of a typical RSG progenitor. We present two models. In the first we use a numerical hydrodynamical profile of a RSG explosion at the beginning of the homologous phase. We then solve the radiation transfer through the expanding gas semi-analytically based on our recombination model. Second, we use an approximated broken power-law for the hydrodynamics and solve for the resulting light curve analytically.

The numerical hydrodynamic profile of the homologous envelope is taken from a simulation of a  $M = 13M_{\odot}$ ,  $R = 840R_{\odot}$  progenitor explosion with  $E = 1.2 \times 10^{51}$  erg (Dessart et al. 2013). We use a snapshot of the hydrodynamic profile before recombination starts at some time during the homologous expansion. Then we construct the properties of the envelope at later times using the fact that it continues to expand freely and cool adiabatically behind the luminosity shell. The light curve is then found by following the dynamics of the luminosity shell, color shell and recombination shell during the homologous expansion. This evolution is governed by the general set of equations (14). These equations can be solved numerically for any  $x_{\text{ion}}(\rho, T)$ ,  $\rho(m)$ ,  $E_{\text{ad}}(m)$  and  $v(m)$ . The explicit equations we solve numerically

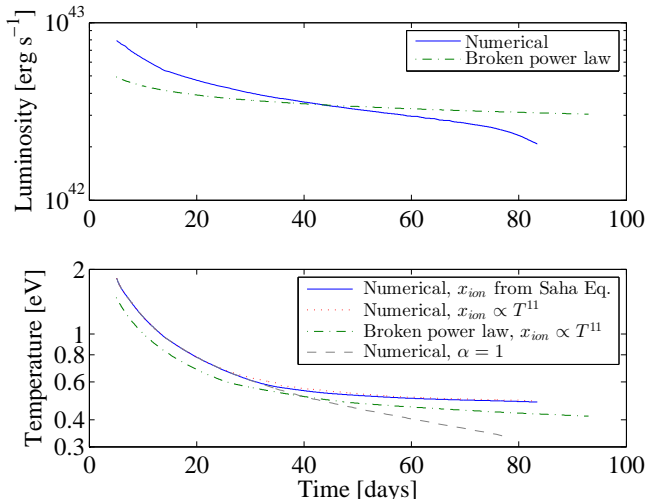


**Figure 5.** The bolometric luminosity and observed temperature for the two examples of RSG explosion described in §6.2. For the envelope taken from numerical simulation, there is no significant difference between the temperature whether we parametrize ionization fraction with the analytical approximation, red dotted line, or with more accurate numerical function according to Saha equation, blue solid line. according to Saha equation. The green dash-dotted line is for the envelope we described analytically using broken power law profiles. The ionization fraction in that case is according to equation (11) with and  $T_{\text{rec}} = 0.6\text{eV}$ . In both examples recombination starts after day  $\sim 30$  and it does not affect the luminosity. The grey dashed line described the solution for the numerical envelope with  $\alpha = 1$ , where recombination has no effect at all.

are based on equations (14) with some correction of pre-factors which were omitted and definitions which were simplified in the analytic model described in the previous sections. The full set of equations are given in appendix B. We solve equations (B1) until the luminosity shell passes  $8M_{\odot}$ . From that point the density profile is roughly constant and our model is not adequate. We consider two different ionization models - (a)  $x_{\text{ion}}(\rho, T)$  according to Saha equation (b)  $x_{\text{ion}} \equiv 1$  (i.e., no recombination). In figure 5 we show the bolometric luminosity and observed temperature as a function of time. These are similar to those observed in some type IIp SNe. In this specific example the color shell does not reach the luminosity shell before most the trapped radiation escapes around day 90, implying that recombination does not affect the bolometric luminosity at all. This is expected based on equation 21, which estimates  $t_L \approx 152$  day. Thus, the bolometric luminosity decreases very slowly with time. Recombination starts at  $\sim$  day 30, and from that time the temperature changes slowly in time. In figures 6, 7 and 8 we show the resulting UV, optical and IR light curves.

The second model we present is fully analytic. The ionization fraction is approximated by a broken power-law,  $x_{\text{ion}} \propto T^{11}$  at  $t < T_{\text{rec}} = 0.6\text{eV}$  (equation 11). We parametrize the envelope of the progenitor as a broken power-law<sup>5</sup> in the following way. The outer part was parametrize with power law profiles, using  $k = 12$  and  $s = 0.9$ . We take this profile according to the profiles pro-

<sup>5</sup> The expressions for luminosity and temperature we provide in §5.1 does not cover the period in which the luminosity shell and color shell propagates inward through different power-law profiles. Nevertheless the relevant expressions can be readily derived.

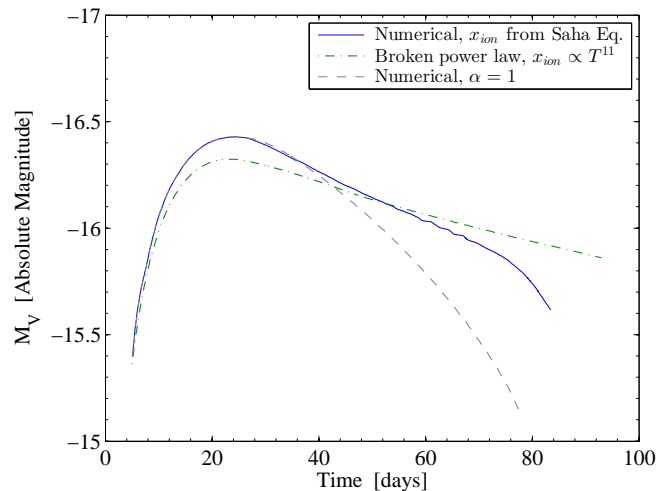


**Figure 6.** Optical V-band light curves ( $5.44 \times 10^{14}$  Hz) for the two examples of RSG explosion described in §6.2. The blue solid line is for the envelope taken from numerical simulation. The ionization fraction for that example is according to Saha equation. The green dash-dotted line is for the envelope we described analytically using broken power law profiles. The ionization fraction in that case is according to equation (11) with  $T_{\text{rec}} = 0.6\text{eV}$ . Recombination starts after day  $\sim 30$ . The grey dashed line described the solution for the numerical envelope with  $\alpha = 1$ , where recombination has no effect.

vided by NS10 for a RSG with  $M = 13M_{\odot}$ ,  $R = 840R_{\odot}$  and  $E = 1.2 \times 10^{51}$  erg. This outer part lies from the surface, inward, up to  $1M_{\odot}$ . From that point inward the density profile is parametrized continuously with  $k = 6$  and  $s = 0.95$ . The reason for this parametrization is that in the numerical envelope we use for the first example we see that  $s = 0.95$  is a good approximation for any  $1M_{\odot} < m$  while  $k = 6$  is a good approximation in the region  $1M_{\odot} < m < 3M_{\odot}$ . At larger masses  $k$  drops continuously (the density profiles becomes shallower). For that reason the analytic solution provides only a rough approximation to a realistic RSG explosion. Nevertheless, the characteristic behavior of the bolometric luminosity and observed temperature is similar to that of the numerical hydrodynamic profile, see figure 5.

The optical and the IR light curves in this example show a slow evolution in time from the onset of recombination at  $\sim$  day 30. This is in agreement with the plateau feature (up to 0.5 in magnitude) seen in observations. The UV light however, which is much more sensitive to small changes in the temperature, drops much faster. Again with agreement with observations. In this example the bolometric luminosity is not affected by recombination. But, in other cases (more compact and/or massive progenitors) the recombination wave is expected to reach the luminosity shell during the plateau phase. A very slow evolution of the optical and IR bands is expected also in that case, with the main difference that the optical light may rise slowly. On the other hand, the slower evolution of the temperature will have a strong effect on the UV light curve which is expected to fall much more slowly, or even rise very slowly, once recombination affect the luminosity. This may explain the late UV plateau observed in some SNe (Bayless et al. 2013).

### 6.3. Plateau Luminosity and Duration

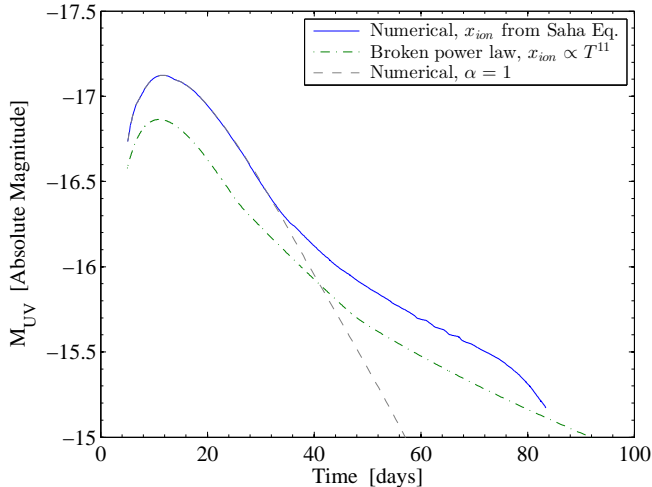


**Figure 7.**  $u$ -band light curves ( $8.33 \times 10^{14}$  Hz) for the two examples of RSG explosion described in §6.2. The lines have the same meaning as in figure 6.

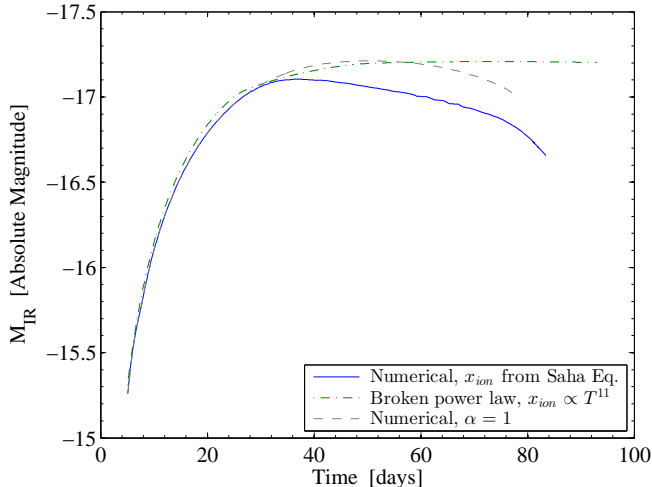


**Figure 8.**  $I$ -band light curves ( $3.33 \times 10^{14}$  Hz) for the two examples of RSG explosion described in §6.2. The lines have the same meaning as in figure 6.

Over the years, much effort has been made in order to connect the observable data to the progenitor and the explosion properties. In type IIP SNe, there have been attempts to relate three observed properties of the SN light curve - the plateau duration, plateau luminosity and photosphere velocity - to three physical properties - the progenitor mass and radius and the explosion energy. Such relations were derived analytically by Arnett (1980) who ignores recombination and by Popov (1993) who uses a step function parameterization with  $\alpha = 0$ . Numerical analysis by Litvinova & Nadezhin (1985) gives results similar to those of Popov (1993).

The plateau duration,  $t_{\text{SN}}$ , can be approximated by the time in which the energy deposited by the shock is released from the *entire* envelope. We examine the energy release by the “last” shell, constituting the bulk of the star. It has a mass  $\sim M_{\text{ej}}$ , radius  $r = v_{\text{SN}} t_{\text{SN}}$  and density  $\sim M_{\text{ej}}/r^3$ , where  $M_{\text{ej}} \sim M$  is the ejected mass and  $v_{\text{SN}} \approx \sqrt{2E/M_{\text{ej}}}$ . If recombination does not affect

the luminosity (i.e.,  $t_L > t_{\text{SN}}$ ), the relations derived by Arnett (1980) are valid:

$$t_{\text{SN}} \propto \frac{M^{0.75} \kappa^{1/2}}{E^{0.25}} \quad t_{\text{SN}} < t_L, \quad (24)$$

$$L_{\text{SN}} \propto \frac{ER}{M\kappa}$$

where  $L_{\text{SN}}$  is the typical luminosity of the plateau

When recombination affects the luminosity, the plateau luminosity and duration can be determined by the following relation

$$E_0 \left( \frac{r}{R_\star} \right)^{-1} t_{\text{SN}}^{-1} \approx L_{\text{SN}} \approx \frac{a T_{\text{cl}}^4 r^3}{x_{\text{ion}}(T_{\text{cl}}) \kappa_T \rho r^2},$$

where  $E_0 \approx E/2$  is the initial internal energy. We use the ionization model according to equation (11) so  $T_{\text{cl}}$  and  $x_{\text{ion}}(T_{\text{cl}})$  should be found by another equation regarding the thermal coupling coefficient of that color shell (equation 14c). Using the above definitions, we find

$$t_{\text{SN}} \propto \frac{M^{0.45} R^{0.23} \kappa^{0.76}}{E^{0.15} T_{\text{rec}}^{0.73}} \quad t_{\text{SN}} > t_L. \quad (25)$$

$$L_{\text{SN}} \propto \frac{E^{0.81} R^{0.54} T_{\text{rec}}^{1.46}}{M^{0.4} \kappa^{0.35}}$$

The general behavior of the scalings we find is rather similar to previous analytical and numerical results (for comparison with scalings from other works see section 7). Therefore, if  $E, R$  and  $M$  are independent, the variation in  $t_{\text{SN}}$  is expected to be larger than the observed, almost constant, plateau duration of 100 days (Arcavi et al. 2012). This implies that there is probably a dependence between these explosion properties (Poznanski 2013).

## 7. COMPARISON TO PREVIOUS WORKS

### 7.1. Analytical Works

A couple of works have dealt with the problem of recombination in SNe envelopes. These works examined a recombination wave which runs inward through the envelope and dictates the energy emission<sup>6</sup>. In these works, recombination divides the envelope into two regions- hot and opaque behind the recombination front, cold and transparent in front of it. The transparent region is characterized with a temperature  $T_2$  and  $\tau(\rho, T_2) = 1$ . The luminosity is  $L = 4\pi R_{\text{ph}}^2 \sigma T_2^4$ , where  $\sigma$  is the Stephan-Boltzmann constant, and  $R_{\text{ph}}$  is the radius of the recombination front which is also the photosphere radius (defined as the point where  $\tau = 1$ ). Thus, the main difference between our work and previous ones is that we examine the coupling between radiation and matter while previous works assume full coupling. In our model we find that  $\tau_{\text{rec-out}}(t) > 1$  for a typical RSG explosion, so the photosphere is located further out from the recombination shell. Moreover, since the recombination shell is also the outermost point in thermal equilibrium, the relation  $L = 4\pi R_{\text{ph}}^2 \sigma T_2^4$  is not valid. In addition, we show that recombination does not affect the luminosity at the onset of recombination. This also comes from the account for coupling between radiation and matter, or more explicitly, the separation between the luminosity

<sup>6</sup> Some works use the term “wave of cooling and recombination” (WCR) or “cooling and recombination wave” (CRW).

shell and the color shell at early times. In the rest of this subsection, we discuss more specifically two fundamental previous works by Grassberg & Nadyozhin (1976) and Popov (1993) which addressed the problem of recombination in SN envelope.

Grassberg & Nadyozhin (1976) examined a recombination wave propagating in a SN envelope. The homologous expanding envelope has a density profile  $\rho \propto r^{-k} t^{k-3}$ , as in our model. They gave a significant role to the energy released from the recombination itself in determining the temperature at the inner region of the recombination wave. Here we shortly summarize their results, focusing on the recombination shell and its boundary conditions. The energy in the internal boundary of the recombination shell is given by  $\chi \rho_{\text{rec}}/m_\mu$ , where  $\chi$  is the recombination potential and  $m_\mu$  is the average mass per ion. The diffusion time in the external boundary is  $\sim r_{\text{rec}}/c$ , since they assume  $\tau_{\text{rec-out}} = 1$ . Equating the luminosity from the external boundary to the release of the energy in the internal boundary during the dynamical time of the shell ( $\sim t$ ) gives

$$\rho/t \propto T_2^4/r_{\text{rec}}.$$

Under the assumption that  $T_2 \approx \text{constant}$ , one finds that  $r_{\text{rec}} \propto t^{\frac{k-4}{k-1}}$ . Since in this analysis  $L \propto r_{\text{rec}}^2$ , then for example  $L \propto t^{0.8}$  for  $k = 6$ . In contrast, we find that the energy from the recombination itself does not play any significant role in determining the dynamics of the recombination shell. Let us consider late times, when  $m_{\text{rec}} = \hat{m}$ . The luminosity released from the internal boundary of the recombination shell, including the energy from recombination, is  $L = E_{\text{ad}}(m_{\text{rec}})/t + \chi \rho_{\text{rec}} r_{\text{rec}}^3/m_\mu t$ . Thus, the recombination energy is important when

$$\frac{\chi}{k_B T_{\text{BB,rec-in}}} \beta_{\text{rec-in}} \gg 1,$$

where  $\beta_{\text{rec-in}}$  is the ratio between gas pressure and radiation pressure in the internal boundary of the shell. We find that this condition is not satisfied,  $\beta_{\text{rec-in}} \sim \frac{k_B T_{\text{rec-in}} \rho_{\text{rec}}}{a T_{\text{rec-in}}^4 m_\mu} \sim 10^{-2} \left( \frac{k_B T_{\text{rec-in}}}{\text{eV}} \right)^{-3}$ . It is only if  $T_{\text{rec-in}} \sim T_{\text{rec}}$  that this inequality may hold. However, this situation does not occur in our solution. In addition, Grassberg & Nadyozhin (1976) found typical values of  $x_{\text{ion}} = 10^{-4} - 10^{-3}$  which is lower than the typical values of  $x_{\text{ion}} \geq 10^{-2}$  found by us and by detailed numerical simulations (see below).

Popov (1993) considered a homogeneous density in the freely expanding envelope. He used an analytic solution by Arnett (1980) who ignores recombination ( $\kappa = \kappa_T$ ). This solution sets conditions before recombination starts that are not realistic in the actual case of a non-homogeneous envelope. The opacity in Popov's model is a step function, such as in equation (A1), with  $\alpha = 0$ . He sets the observed temperature to be  $T_2 = T_{\text{rec}}$  from the onset of recombination so the recombination wave has a zero width<sup>7</sup>. We find that if  $\alpha = 0$ , then at the onset of recombination there is a sharp increase in the luminosity (follows a discontinuity in the evolution). This

<sup>7</sup> Popov's model does not deal with color temperature and coupling between matter and radiation, so the onset of recombination is defined by the time when the temperature at the photosphere is  $T_{\text{rec}}$ .

phenomena is not seen in Popov's solution. However, we can not give a fair comparison between the evolution of the luminosity and observed temperature derived above and those derived by Popov, since he treated a problem with homogeneous density which we do not consider here. Nevertheless, the relations that Popov finds for the plateau duration and luminosity are not very different than our relations when recombination plays a role:

$$\begin{aligned} t_{\text{SN,Popov}} &\propto \frac{M^{1/2} R^{1/6} \kappa^{1/6}}{E^{1/6} T_{\text{rec}}^{2/3}} \\ L_{\text{SN,Popov}} &\propto \frac{E^{5/6} R^{2/3} T_{\text{rec}}^{4/3}}{M^{1/2} \kappa^{1/3}} \end{aligned} \quad (26)$$

## 7.2. Numerical Works

Our results regarding the propagation of a recombination wave in the ejected envelope of a RSG are compatible with the picture that is found in numerical studies. Those studies examine the photometric and spectroscopic evolution of SNe, from the initial pulse up to the nebular phase. They find, similarly to our model, that recombination takes place over a small mass scale (much smaller than  $m_{\text{rec}}$ ). The radiation and gas temperature are coupled in the ionized region and they remain coupled while they drop significantly within the recombination shell. Once the temperature falls to the observed temperature the gas and the radiation decouple and the gas continues to cool while the radiation temperature is constant (e.g., Utrobin 2007). Quantitatively, the main result of our model that can be compared to the published results of numerical simulations is the ionization level at the point that the radiation observed temperature is determined (i.e.,  $x_{\text{ion}}(T_{\text{cl}})$ ). For typical RSG parameters our model (using equation 11) predicts  $x_{\text{ion}}(T_{\text{cl}}) \approx 0.05$  at  $t = 100$  day. This value agrees with numerical models that properly include the radiation-gas coupling (e.g., Utrobin 2007; Kasen & Woosley 2009), which find that the ionization fraction at the external boundary of the recombination shell is  $\approx 10^{-2} - 10^{-1}$ . It also explains the physical origin of the ‘‘opacity floor’’, which is invoked in order to fit the observations in numerical simulations that do not treat the coupling properly (e.g., Young 2004; Bersten et al. 2011). The typical value for this floor in hydrogen rich material is  $0.01 \text{ cm}^2 \text{ gr}^{-1}$ , which corresponds to  $x_{\text{ion}} = 0.03$ . Another related prediction of our model is that the observed temperature falls from  $T_{\text{rec}} = 6,500 - 7,000 \text{ K}$  at the time that recombination starts to  $5,000 - 6,000 \text{ K}$  by the time that it ends. This is similar to the values obtained in numerical simulations.

## 8. SUMMARY AND DISCUSSION

We study analytically the effect of recombination on the evolution of SNe light curves. The process of recombination reduces the number of free electrons, reducing both the opacity and the radiation-gas coupling (via the ability of the gas to absorb and emit photons). The balance between the two, opacity and coupling, is what determines the radiation temperature and ionization level in the recombined gas. Once recombination starts a wave of recombination, which is followed by cooling, starts to propagate inward through the envelope.

We develop a model which describes the properties of the relevant shells of the envelope- the shells which dominates the bolometric luminosity and the observed tem-

perature. The concept of the model is to consider three characteristic shells which dominate the light curves: (1) The luminosity shell, which is the source of the observed luminosity. This shell determines the radiative flux through all the shells external to it. (2) The color shell which is the outermost shell in which photons can be thermalized over the diffusion time. This shell dictates the color of the observed temperature. (3) The recombination shell which is the shell where recombination takes place. It is the outermost shell which is fully ionized on its inner boundary and it is highly recombined on its outer boundary. We proved that this shell coincides with the color shell once recombination starts and at late times it also coincides with the luminosity shell. The main advantage of our model over previous analytical studies of the process is that it takes into account the coupling between the radiation and the gas, which is found to be crucial in finding the ionization level at the point where the observed temperature is determined. It can, therefore, provide a reliable estimate of the evolution of the observed temperature and of the bolometric luminosity. Our model provides new insight into the recombination process and to the relations between the observables and the progenitor and explosion properties.

We find that when recombination starts it first affects only the temperature, which becomes almost constant with time. The bolometric luminosity, at first, continues to drop very slowly without being affected by recombination. Only later the recombination wave reaches the luminosity shell. The temperature from that point evolves even more slowly, while the bolometric luminosity stops dropping or even rises slowly. The effect of this transition is rather mild in the optical but it should cause significant flattening of the UV light. Whether the recombination wave reaches the luminosity shell before the end of the plateau depends on the progenitor properties (e.g., it is more likely to take place in less extended progenitors). We farther find that the radiation-gas coupling limit the drop of the ionization fraction in the recombination shell to 0.01-0.1. This in turn is the origin of

the very slow drop in the observed temperature, which is  $T_{\text{rec}} = 6,500 - 7,000$  K when recombination starts and  $5,000 - 6,000$  K when the plateau ends.

Another interesting result of our analysis is that the observed plateau is not a generic property of the propagation of a recombination wave in expanding ionized gas. The generic property is the much slower evolution of the observed temperature once recombination starts (due to the strong feedback of the temperature drop on the coupling). This fixes the observed temperature around the  $R$  and  $I$  bands. However, the slow evolution of the bolometric luminosity is a result of the typical hydrodynamical structure of exploding stellar envelopes. Different structures can result in a much faster decay or rise of the bolometric luminosity. Slightly different stellar structures is probably the main source of the various behaviors seen in type IIP SNe.

The derivation of a fully analytical solution requires the following approximations- (1) power-law profile for the density and adiabatic cooling at late times; (2) neglecting the density dependence in the ionization fraction; (3) power-law relation between the ionization fraction and the temperature; (4) neglecting radioactive energy from  $^{56}\text{Ni}$ ; (5) assuming free-free as the most efficient process for photon production. However, the basic ideas of our model- (1) separation of the envelope into successive shells; (2) finding the recombination shell by the properties of its boundaries, can be used for more general assumptions than (1)-(6) above, as is described in appendix B. The simple equations introduced in (B1) can be extended even further by changing the function  $\eta$  such that it includes bound-free process or by adding energy from radioactive decay. Hence, our model serve as a simple tool to examine the effect of some basic mechanisms on the evolution of SNe light curves.

This research was partially supported by an ERC starting grant, ISF and ISA grants, and an iCore center. We thank Roni Waldman and Eli Livne for providing us an example of a numerical stellar envelope.

## APPENDIX

### A. IONIZATION FRACTION AS A STEP FUNCTION

Consider the following parametrization

$$x_{\text{ion}} = \begin{cases} 1 & T > T_{\text{rec}} \\ \alpha & T < T_{\text{rec}} \end{cases}, \quad (\text{A1})$$

where  $0 \leq \alpha < 1$ . As opposed to the description in §4.2, now the opacity does not drop with the temperature for  $T < T_{\text{rec}}$ . Therefore the recombination shell is not necessarily coupled to the color shell and equations (14b)-(14c) are not valid. The dynamics of the luminosity shell is still dictated by equation (14a) and the color shell is simply defined by

$$\begin{cases} \eta(m_{\text{cl}}, t) = 1 & , \text{ if } m_{\text{cl}} < m_{\text{rec}} \\ m_{\text{cl}} = m_{\text{rec}} & , \text{ otherwise} \end{cases}. \quad (\text{A2})$$

In §A.1, we find the dynamics of the recombination shell and by doing so, we also find the evolution of the bolometric luminosity. In §A.2 we discuss the dynamics of the color shell and find the evolution of the observed temperature for the different scenarios. It is quite cumbersome to describe all the different scenarios of the evolution. Nevertheless, the description below gives a complete picture and the main results and equations. In order to illustrate the various scenarios we summarize the evolution in table A1. In the following analysis we use the notation  $t_{\text{rec}}^{\pm}$  to emphasize the discontinuity at the onset of recombination. It is evident from the following analysis that the dynamics of the recombination shell and the color shell are continuous in  $\alpha$ . Thus, for any choice of  $\alpha$ , a unique solution for the evolution is found.

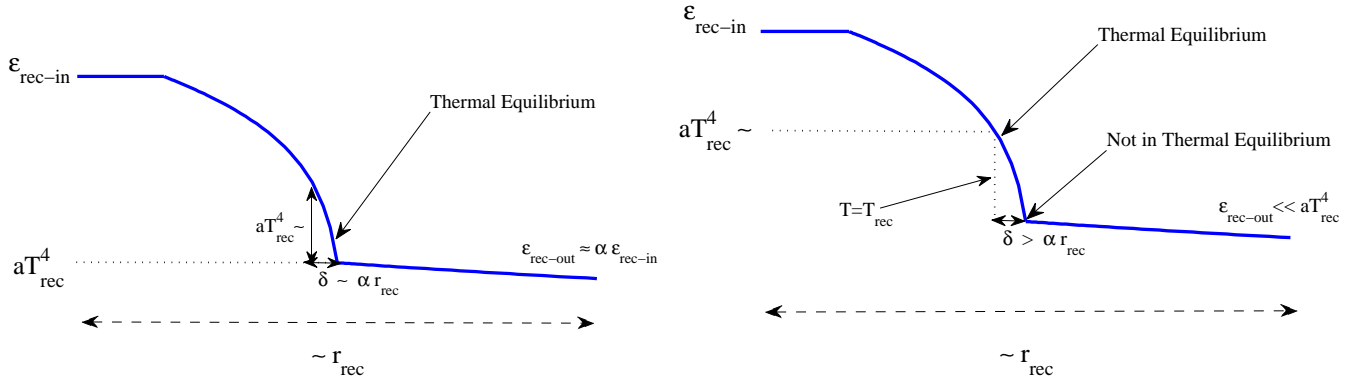


**Figure A1.** Schematic description of the energy density profile (logarithmic scale) inside the recombination shell when  $m_{\text{rec}} = \hat{m}$  for the step function model, shown for two different scenarios: When the radiation behind  $T = T_{\text{rec}}$  is in thermal equilibrium (**left**) and when it is not (**right**), according to §A.1. **In the left panel:** Behind the point with  $T = T_{\text{rec}}$  in a subshell with a width of  $\delta \sim \alpha r_{\text{rec}}$  the energy density is approximately  $aT_{\text{rec}}^4$ . The external boundary is not necessarily in thermal equilibrium, see §A.2. However, the energy density there is  $\sim aT_{\text{rec}}^4$ . **In the right panel:** The radiation departs from thermal equilibrium in a subshell with a width of  $\delta > \alpha r_{\text{rec}}$  located behind the point where  $T = T_{\text{rec}}$ . The energy density in this subshell is approximately  $aT_{\text{rec}}^4$ . From the point in which the radiation departs from thermal equilibrium out to the point where  $T = T_{\text{rec}}$ , the energy density decreases significantly while the temperature is roughly constant  $\sim T_{\text{rec}}$ . From the point with  $T = T_{\text{rec}}$  outward the profiles of the energy density and the temperature are approximately homogeneous. In both cases, the luminosity in the discussed subshells is determined by the luminosity in internal region.

### A.1. Dynamics of the Recombination Shell

Consider the recombination shell at  $t > t_{\text{rec}}$ . In the internal boundary we have  $\eta_{\text{rec-in}} < 1$  and  $\epsilon_{\text{rec-in}} > aT_{\text{rec}}^4$ . As we go further out, but still within the shell, toward the point where  $T = T_{\text{rec}}$ , the energy density and the thermal coupling decrease significantly. For  $T \leq T_{\text{rec}}$  all the hydrodynamic properties change on a scale of  $r_{\text{rec}}$ , thus, from the point where  $T = T_{\text{rec}}$  up to the external boundary they can be approximated as homogeneous. Schematic profile inside the recombination shell is given in figures 2 and A1. We need to understand the conditions at a small subshell behind the point with  $T = T_{\text{rec}}$ . The width of this subshell is the scale on which there is no significant change in the characteristic of this subshell. Let us take a distance  $\delta$  inward from the point with  $T = T_{\text{rec}}$ , and consider a subshell with width  $\delta$ . The optical depth and the diffusion time of this subshell are given by

$$\tau(\delta) = \kappa_T \rho_{\text{rec}} r_{\text{rec}} \left( \frac{\delta}{r_{\text{rec}}} \right) \quad , \quad t_d(\delta) = \frac{\kappa_T \rho_{\text{rec}} r_{\text{rec}}^2}{c} \left( \frac{\delta}{r_{\text{rec}}} \right)^2 \quad . \quad (\text{A3})$$

According to equation (9), the thermal coupling coefficient of this subshell is

$$\eta(\delta) = \left( \frac{\epsilon(\delta)}{\epsilon_{\text{cl}}(t_{\text{rec}})} \right)^{7/8} \left( \frac{\rho_{\text{rec}}}{\rho_{\text{cl}}(t_{\text{rec}})} \right)^{-3} \left( \frac{r_{\text{rec}}}{r_{\text{cl}}(t_{\text{rec}})} \right)^{-2} \left( \frac{\delta}{r_{\text{rec}}} \right)^2 \quad . \quad (\text{A4})$$

Note that we consider only subshells with  $\delta \gtrsim \alpha r_{\text{rec}}$ . The subshell with  $\delta \sim \alpha r_{\text{rec}}$  is the smallest subshell which can be considered with homogeneous properties. The luminosity in the external boundary of the recombination shell and in the subshell is dictated by internal regions. The equation which governs the dynamic of the recombination shell is

$$\frac{\epsilon_{\text{rec-out}} c r_{\text{rec}}}{\alpha \kappa_T \rho_{\text{rec}}} = \frac{E_{\text{ad}}(\hat{m})}{t} = \frac{\epsilon(\delta) r_{\text{rec}}^3 \left( \frac{\delta}{r_{\text{rec}}} \right)}{t_d(\delta)} \quad , \quad (\text{A5})$$

where  $\delta$  or  $\epsilon_{\text{rec-out}}$  should be determined. If the change in the opacity is not too large then the radiation is in thermal equilibrium at least up to the point where  $T = T_{\text{rec}}$ . More precisely, there is a critical value, denoted with  $\alpha_0$ , such that for  $\alpha > \alpha_0$  this is true at the onset of recombination. Hence, we divide our analysis of the dynamics of the recombination shell in to two different scenarios- when the radiation behind  $T = T_{\text{rec}}$  is in thermal equilibrium and when it is not. We emphasize here that the condition of thermal equilibrium behind  $T = T_{\text{rec}}$  means that the energy density at the point where  $T = T_{\text{rec}}$  is  $aT_{\text{rec}}^4$ .

Consider the first scenario, from the continuity of the energy density, we know that the energy density at the external region is also roughly  $aT_{\text{rec}}^4$ . Hence,  $\epsilon_{\text{rec-out}} \approx aT_{\text{rec}}^4$ . Using this to solve the left equality in equation (A5) for  $m_{\text{rec}}(t)$

we find

$$m_{\text{rec}}(t) = \begin{cases} m_{\text{cl}}(t_{\text{rec}}^-) \alpha^{-\frac{k-3}{k+1}} \left(\frac{t}{t_{\text{rec}}}\right)^{\frac{2(k-3)(-(k-3)s+3k-7)}{(k+1)(k-2)}} & , m_{\text{rec}} < \hat{m} \\ \hat{m}(t_{\text{rec}}^-) \left(\frac{\alpha}{\alpha_L}\right)^{-\frac{k-3}{(k-3)s+k+2}} \left(\frac{t}{t_{\text{rec}}}\right)^{\frac{6k-18}{(k-3)s+k+2}} & , m_{\text{rec}} = \hat{m} \end{cases} \propto \begin{cases} t^{1.75} & , m_{\text{rec}} < \hat{m} \\ t^{1.66} & , m_{\text{rec}} = \hat{m} \end{cases}, \quad (\text{A6})$$

where

$$\alpha_L = \Delta^{\frac{k+1}{k-3}} \approx \Delta^{2.33}. \quad (\text{A7})$$

As is expected, at  $t_{\text{rec}}$  there is a discontinuity in the recombination shell mass and afterwards recombination continues to reach deeper shells. If the change in the opacity is large, that is  $\alpha$  is lower than the critical value  $\alpha_L$ , then the recombination shell can affect the luminosity from the onset of recombination. This scenario is defined by the condition  $m_{\text{rec}}(t_{\text{rec}}^+) > \hat{m}(t_{\text{rec}}^-)$ . This condition implies that the recombination shell is also the luminosity shell from the onset of recombination. If  $\alpha > \alpha_L$ , the recombination shell moves rapidly inward, so finally at some time  $t = t_L$  it reaches to the luminosity shell. The value of  $t_L$  is defined by  $m_{\text{rec}}(t_L) = \hat{m}(t_L)$ , where  $m_{\text{rec}}$  is given by the first expression in equation (A6),

$$t_L = \left(\frac{\alpha}{\alpha_L}\right)^{-\frac{k-2}{2((k-3)s-2k+8)}} t_{\text{rec}} \approx \left(\frac{\alpha}{\alpha_L}\right)^{1.74} t_{\text{rec}}. \quad (\text{A8})$$

The expression for the bolometric luminosity is

$$L(t) = L(t_{\text{rec}}^-) \begin{cases} \left(\frac{t}{t_{\text{rec}}}\right)^{-\frac{2(1-s)(k-3)}{k-2}} \\ L(t_{\text{rec}}^-) \left(\frac{\alpha}{\alpha_L}\right)^{-\frac{(k-3)s+1}{(k-3)s+k+2}} \left(\frac{t}{t_{\text{rec}}}\right)^{-\frac{2(-2(k-3)s+k-1)}{(k-3)s+k+2}} \end{cases} \propto \begin{cases} t^{-0.07} & , m_{\text{rec}} < \hat{m} \\ \alpha^{-0.35} t^{0.13} & , m_{\text{rec}} = \hat{m} \end{cases}. \quad (\text{A9})$$

Equation (A9) gives us the discontinuity in the luminosity at  $t_{\text{rec}}$  for the case where  $\alpha < \alpha_L$ . For  $\alpha > \alpha_L$  the luminosity is continuous throughout the whole evolution.

For completeness, we examine the times and values of  $\alpha$  in which the solution given in (A6) is relevant. In order to check the consistency of the solution above we assume that the energy density in a small subshell behind  $T = T_{\text{rec}}$  is  $aT_{\text{rec}}^4$  and check whether  $\eta(\delta) < 1$ . Taking  $\epsilon(\delta) = aT_{\text{rec}}^4$  and  $\epsilon_{\text{rec-out}} = aT_{\text{rec}}^4$ , equation (A5) reads  $\delta = \alpha r_{\text{rec}}$ . Using this and  $m_{\text{rec}}(t)$  from equation (A6) in equation (A4), we find

$$\eta(\delta = \alpha r_{\text{rec}}) = \begin{cases} \alpha^{\frac{k-4}{k+1}} \left(\frac{t}{t_{\text{rec}}}\right)^{\frac{(k-3)(2(3k-2)s-11k+14)}{(k-2)(k+1)}} \\ \left(\frac{\alpha}{\alpha_0}\right)^{-\frac{2(k-3)s-k+6}{(k-3)s+k+2}} \left(\frac{t}{t_{\text{rec}}}\right)^{\frac{7(k-3)s-11k+26}{(k-3)s+k+2}} \end{cases} \approx \begin{cases} \alpha^{0.28} \left(\frac{t}{t_{\text{rec}}}\right)^{-2.31} & m_{\text{rec}} < \hat{m} \\ \left(\frac{\alpha}{\alpha_0}\right)^{-0.52} \left(\frac{t}{t_{\text{rec}}}\right)^{-1.85} & m_{\text{rec}} = \hat{m} \end{cases}, \quad (\text{A10})$$

where expression for  $\alpha_0$  is

$$\alpha_0 = \Delta^{\frac{(3k-2)(s(k-3)+1)}{(k-3)(2(k-3)s-k+6)}} \approx \Delta^{3.6}. \quad (\text{A11})$$

From equation (A10) we conclude that when  $m_{\text{rec}} < \hat{m}$  then the region behind  $T = T_{\text{rec}}$  is in thermal equilibrium. In addition, for  $\alpha > \alpha_0$ , the radiation behind  $T = T_{\text{rec}}$  is in thermal equilibrium at the onset of recombination and it keeps to be in thermal equilibrium throughout the whole evolution. This is because  $\eta(\delta = \alpha r_{\text{rec}}) < 1$  for  $t > t_{\text{rec}}$ . Hence, the solution in equation (A6) is consistent from the onset of recombination if  $\alpha > \alpha_0$ . If  $\alpha < \alpha_0$  it is consistent from  $t = t_1$  defined by  $\eta(\delta = \alpha r_{\text{rec}})(t_1) = 1$

$$t_1 = \left(\frac{\alpha}{\alpha_0}\right)^{\frac{2(k-3)s-k+6}{7(k-3)s-11k+6}} t_{\text{rec}} \approx \left(\frac{\alpha}{\alpha_0}\right)^{-0.28} t_{\text{rec}}. \quad (\text{A12})$$

Next, we provide the dynamics of the recombination shell under the assumption that the radiation is out of thermal equilibrium behind  $T = T_{\text{rec}}$ . According to the result above, we consider only the situation in which  $m_{\text{rec}} = \hat{m}$ , since since  $\alpha_0 < \alpha_L$ . The radiation goes out of thermal equilibrium somewhere between the internal boundary of the recombination shell to the point where  $T = T_{\text{rec}}$ . Let us say that this transition appears in a subshell located inward to the point where  $T = T_{\text{rec}}$ , with  $\delta > \alpha r_{\text{rec}}$ . The temperature in this subshell is a black body temperature,  $T_{\text{cl}}$ . We can take  $T_{\text{cl}} \approx T_{\text{rec}}$ , since from this subshell out to where  $T = T_{\text{rec}}$  the radiation is out of thermal equilibrium and therefore can barely change the temperature. On the other hand the energy density at the external boundary is much lower than  $aT_{\text{rec}}^4$ . This is the main difference between the case in which the radiation behind  $T = T_{\text{rec}}$  is thermalized and when it is not, see figure A1. Taking  $\epsilon(\delta) = aT_{\text{rec}}^4$ , the right equality in equation (A5) and the requirement  $\eta(\delta) = 1$  are solved for  $m_{\text{rec}}(t)$  and  $\delta(\eta = 1)$ . We find the expressions for the dynamics of the recombination shell and the

bolometric luminosity,

$$\hat{m}(t) = m_{\text{rec}}(t) = \hat{m}(t_{\text{rec}}^-) \Delta^{-\frac{k-4}{2(k-3)s-k+6}} \left(\frac{t}{t_{\text{rec}}}\right)^{\frac{5(k-3)}{2(k-3)s-k+6}} \approx \hat{m}(t_{\text{rec}}^-) \Delta^{-1.35} \left(\frac{t}{t_{\text{rec}}}\right)^{2.63}, \quad (\text{A13})$$

$$L(t) = L(t_{\text{rec}}^-) \Delta^{-\frac{(k-4)((k-3)s+1)}{(k-3)(2(k-3)s-k+6)}} \left(\frac{t}{t_{\text{rec}}}\right)^{\frac{(k-3)s+2k-7}{2(k-3)s-k+6}} \approx L(t_{\text{rec}}^-) \Delta^{-0.45} \left(\frac{t}{t_{\text{rec}}}\right)^{1.38}. \quad (\text{A14})$$

The luminosity and the mass of the recombination shell given in (A13) and (A14) do not depend on the value of  $\alpha$ . This is because we assume that the outermost point in thermal equilibrium is in a subshell characterized with  $\delta(\eta = 1) > \alpha r_{\text{rec}}$ . For such subshell the optical depth and the diffusion time do not depend on the value of  $\alpha$ . The width of this subshell is

$$\delta(\eta = 1) = \alpha_0 \left(\frac{t}{t_{\text{rec}}}\right)^{-\frac{-7(k-3)s+11k-26}{2(k-3)s-k+6}} r_{\text{rec}} \approx \alpha_0 \left(\frac{t}{t_{\text{rec}}}\right)^{-3.52} r_{\text{rec}}, \quad (\text{A15})$$

where the value of  $\alpha_0$  is given in equation (A11). To conclude, for  $\alpha < \alpha_0$ , at the onset of recombination the radiation behind  $T = T_{\text{rec}}$  is out of thermal equilibrium and the dynamics of the recombination shell is given by equation (A13). As time progresses, we find that  $\delta(\eta = 1)/r_{\text{rec}}$  decreases and that the coupling in this shell increases. Once  $\delta(\eta = 1) = \alpha r_{\text{rec}}$  the radiation behind  $T = T_{\text{rec}}$  is thermalized and the evolution of the recombination shell and the luminosity is given by equations (A6) and (A9). The time in which this transition occurs is  $t_1$  given in equation (A12). For  $\alpha = 0$  we see that  $t_1 \rightarrow \infty$  so the evolution of the luminosity is given by (A14) for  $t > t_{\text{rec}}$ .

We note here that for small values of  $\alpha$ , it is possible (depending on the initial conditions) that the optical depth in the relevant regions is lower than 1. In that case, our analysis is not consistent. However, since the step function model, especially with low values of  $\alpha$ , is not physical, we do not discuss here how the analysis should be modified in the case of such inconsistency. In addition, for large values of  $\alpha$  it is possible that  $m_{\text{rec}} > \hat{m}$ , as opposed to the continuous model. As recombination reaches deeper shell the temperature at the internal boundary decreases. Once  $T_{\text{rec-in}} = T_{\text{rec}}$ , or equivalently  $c/v(m_{\text{rec}}) = \tau_{\text{rec-out}}$ , the evolution is the same as before recombination starts, only now the opacity is  $\alpha\kappa_T$  instead of  $\kappa_T$ . We mark with  $\tilde{t}$  the time from which this scenario holds.

## A.2. Color Temperature

We have already seen that there are several scenarios for the evolution of the bolometric luminosity, depending on the initial condition when recombination starts. The evolution of the color temperature also shows various scenarios. When  $\alpha < \alpha_0$  during the time  $t_{\text{rec}} < t < t_1$  the outermost point in thermal equilibrium is located behind the point of  $T = T_{\text{rec}}$  and we have approximated that  $T_{\text{cl}} \approx T_{\text{rec}}$ . In this case the recombination shell is also the last shell which is in thermal equilibrium, so  $m_{\text{rec}} = m_{\text{cl}}$ . Moreover, for  $\alpha = 0$  the color temperature is  $T_{\text{rec}}$  throughout the whole evolution ( $t_1 \rightarrow \infty$ ). This is simply because  $\alpha = 0$  means that there are no free electrons for  $T < T_{\text{rec}}$  so there are no efficient processes which can change the temperature external to the point where  $T = T_{\text{rec}}$ . On the other hand, when the radiation behind the point with  $T = T_{\text{rec}}$  is in thermal equilibrium, the color temperature may drop below  $T_{\text{rec}}$ . It depends whether shells external to the recombination shell generate enough photons through free-free emission such that the radiation is in thermal equilibrium.

We find that for any choice of  $\alpha$ , at the onset of recombination the external boundary of the recombination shell is not in thermal equilibrium, therefore for  $t = t_{\text{rec}}^+$  the observed temperature is  $T_{\text{rec}}$ . As we continue with the evolution of  $m_{\text{rec}}$  the coupling in the external boundary increases and once  $\eta_{\text{rec-out}} = 1$ , the color shell starts to move outward from the recombination shell. From that point, the color temperature starts to decrease and  $m_{\text{cl}}(t) < m_{\text{rec}}(t)$ . The color shell in that case can be found by requiring  $\eta(m_{\text{cl}} < m_{\text{rec}}) = 1$ . The color temperature is found by using equation (7) and (8). In table A1 we add more information about the times of transitions between different types of evolution. For example, the times  $\bar{t}_1$  and  $\bar{t}_2$  in which the color shell is external to the recombination shell and the temperature drops below  $T_{\text{rec}}$ , or the critical value  $\alpha_1$ , such that for  $\alpha > \alpha_1$  the temperature drops below  $T_{\text{rec}}$  before the luminosity changes due to recombination. Figures 3 and 4 show the evolution in time of the bolometric luminosity and observed temperature for various values of  $\alpha$ .

## B. EQUATIONS FOR THE SEMI-ANALYTICAL SOLUTION

We take the profiles  $\rho_i = \rho(m, t_i)$ ,  $E_{\text{ad},i} = E_{\text{ad}}(m, t_i)$ ,  $r_i = r(m, t_i)$  and  $v(m)$  at some early time  $t_i$  before recombination starts and consider all the shells which already reached their coasting velocity (spherical phase). We defined the following properties of each shell

$$\tau_i(m) = \int_{r_i}^{\infty} \kappa_T \rho_i dr'_i, \quad t_{d,i}(m) = \int_{r_i}^{\infty} \frac{3\tau_i}{c} dr'_i,$$

We construct the profiles at later times,  $t > t_i$ , if there was *no recombination*.

$$\rho(m, t) = \rho_i \left( \frac{t}{t_i} \right)^{-3}, \quad E_{\text{ad}}(m, t) = E_{\text{ad},i} \left( \frac{t}{t_i} \right)^{-1}, \quad t_d(m, t) = t_{d,i} \left( \frac{t}{t_i} \right)^{-1},$$

$$\eta(m, t, T) = \frac{7 \times 10^5 \text{s}}{t_d} \left( \frac{\rho}{10^{-10} \text{g cm}^{-3}} \right)^{-2} \left( \frac{k_B T}{100 \text{eV}} \right)^{7/2}.$$

The equation for  $\eta$  is according to equation 9 in NS10. Then, we solve the following equations, which represent the basic equations (14), for  $\hat{m}(t)$ ,  $m_{\text{cl}}(t)$  and  $T_{\text{cl}}(t)$ .

$$\begin{cases} t_d(\hat{m}, t) = t & , \text{ if } \hat{m} > m_{\text{cl}} \\ \hat{m} = m_{\text{rec}} & , \text{ otherwise} \end{cases}, \quad (\text{B1a})$$

$$\frac{E_{\text{ad}}(\hat{m}, t)}{t} = \frac{a T_{\text{cl}}^4 \frac{m_{\text{cl}}}{\rho_{\text{cl}}}}{x_{\text{ion}}(\rho_{\text{cl}}, T_{\text{cl}}) t_d(m_{\text{cl}}, t)}, \quad (\text{B1b})$$

$$\eta(m_{\text{cl}}, t, T_{\text{cl}}) x_{\text{ion}}(\rho_{\text{cl}}, T_{\text{cl}})^{-3} = 1, \quad (\text{B1c})$$

where  $\rho_{\text{cl}} = \rho(m_{\text{cl}}, t)$ . When  $x_{\text{ion}} \neq 1$  the color shell is the recombination shell. The luminosity is given by  $L = E_{\text{ad}}(\hat{m}, t)/t$ . In §6.2 we present the solution for two models of the ionization fraction-  $x_{\text{ion}}$  is given by equation (11) and  $x_{\text{ion}}(\rho, T)$  is given by Saha equation.

## C. $^{56}\text{Ni}$ LUMINOSITY

Here we consider the luminosity due to  $^{56}\text{Ni}$  decay. We focus on the relevance of the decay process as a source of energy. We do not discuss its effect on the opacity. The signal from SNe explosions is dominated by two sources of energy- the shocked medium and the radioactive decay  $^{56}\text{Ni} \rightarrow ^{56}\text{Co}$ . We compare between these two sources during the plateau. We consider the last shell which releases its energy. The energy due to the shock is calculated in §6.3 above,

$$E_0 \left( \frac{v_{\text{SN}} \cdot t_{\text{SN}}}{R_{\star}} \right)^{-1}.$$

The energy from the radioactive decay is given by the adiabatic cooling of the radioactive decay energy which is emitted from  $t = 0$  up to  $t = t_{\text{SN}}$ . It can be approximated by

$$\epsilon_{56} \cdot \tau_{56} \left( \frac{\tau_{56}}{t_{\text{SN}}} \right) M f_{56}(M),$$

where  $M \approx 0.5M_{\star}$ ,  $f_{56}$  is the fraction of  $^{56}\text{Ni}$  in this shell,  $\epsilon_{56} = 3.9 \times 10^{10}$  is the energy per unit mass per unit time released by the decay and  $\tau_{56} = 8.76$  days is the half time of the decay. Whether the energy emission from  $^{56}\text{Ni}$  decay affect the plateau or not depends on the radius of the pre-SN, the explosion energy and the  $^{56}\text{Ni}$  mixing in the envelope. We take  $t_{\text{SN}} = 120$  days as the end of the plateau and assume for simplicity that  $f_{56} = 0.1$ . The energy of the shocked medium is  $\approx 10^{48} \text{erg} E_{51}^{0.5} R_{500} M_{15}^{0.5}$  and the energy from  $^{56}\text{Ni}$  decay is  $\approx 2 \times 10^{47} \text{erg} M_{15}$ . Hence, the plateau feature in a typical RSG explosion is not affected by the energy release from  $^{56}\text{Ni}$ .

## D. GLOSSARY OF MAIN SYMBOLS AND NOTATIONS

1.  $t$ : time since breakout.
2.  $r$ : radius.
3.  $v$ : velocity.
4.  $m(r)$ : mass which lies external to the radius  $r$ .
5.  $\rho$ : mass density.
6.  $E_{\text{ad}}$ : internal energy of a shell due to adiabatic expansion.
7.  $t_d$ : diffusion time.

$0 \leq \alpha < \alpha_0$				
Time	$t_{\text{rec}} < t < t_1$	$t_1 \leq t < \bar{t}_1$	$\bar{t}_1 \leq t < \tilde{t}$	$t > \tilde{t}$
Evolution	$\hat{m} = m_{\text{rec}} = m_{\text{cl}}$	$\hat{m} = m_{\text{rec}} = m_{\text{cl}}$	$\hat{m} = m_{\text{rec}} > m_{\text{cl}}$	$\hat{m} > m_{\text{rec}} > m_{\text{cl}}$
Luminosity	affected	affected	affected	affected
Observed temperature	$T_{\text{rec}}$	$T_{\text{rec}}$	$< T_{\text{rec}}$	$< T_{\text{rec}}$

$\alpha_0 \leq \alpha < \alpha_L$			
Time	$t_{\text{rec}} \leq t < \bar{t}_1$	$\bar{t}_1 \leq t < \tilde{t}$	$t > \tilde{t}$
Evolution	$\hat{m} = m_{\text{rec}} = m_{\text{cl}}$	$\hat{m} = m_{\text{rec}} > m_{\text{cl}}$	$\hat{m} > m_{\text{rec}} > m_{\text{cl}}$
Luminosity	affected	affected	affected
Observed temperature	$T_{\text{rec}}$	$< T_{\text{rec}}$	$< T_{\text{rec}}$

$\alpha_L \leq \alpha < \alpha_1$				
Time	$t_{\text{rec}} \leq t < t_L$	$t_L \leq t < \bar{t}_1$	$\bar{t}_1 \leq t < \tilde{t}$	$t > \tilde{t}$
Evolution	$\hat{m} > m_{\text{rec}} = m_{\text{cl}}$	$\hat{m} = m_{\text{rec}} = m_{\text{cl}}$	$\hat{m} = m_{\text{rec}} > m_{\text{cl}}$	$m_{\text{rec}} > \hat{m} > m_{\text{cl}}$
Luminosity	not affected	affected	affected	affected
Observed temperature	$T_{\text{rec}}$	$T_{\text{rec}}$	$< T_{\text{rec}}$	$< T_{\text{rec}}$

$\alpha_1 \leq \alpha \leq 1$				
Time	$t_{\text{rec}} \leq t < \bar{t}_2$	$\bar{t}_2 \leq t < t_L$	$t_L \leq t < \tilde{t}$	$t > \tilde{t}$
Evolution	$\hat{m} > m_{\text{rec}} = m_{\text{cl}}$	$\hat{m} > m_{\text{rec}} > m_{\text{cl}}$	$\hat{m} = m_{\text{rec}} > m_{\text{cl}}$	$m_{\text{rec}} > \hat{m} > m_{\text{cl}}$
Luminosity	not affected	not affected	affected	affected
Observed temperature	$T_{\text{rec}}$	$< T_{\text{rec}}$	$< T_{\text{rec}}$	$< T_{\text{rec}}$

$\alpha_0$  - for lower values of  $\alpha$  the evolution is similar to  $\alpha = 0$  at  $t_{\text{rec}} < t < t_1$ .

$t_1$  - from that time the radiation behind the point where  $T = T_{\text{rec}}$  is in thermal equilibrium.

$\bar{t}_1$  - the time when the color temperature drops below  $T_{\text{rec}}$ , when  $\hat{m} = m_{\text{rec}}$ .

$\alpha_L$  - for  $\alpha < \alpha_L$  the recombination shell is the luminosity shell when recombination starts.

$t_L$  - when  $\alpha > \alpha_L$  this is the time when  $m_{\text{rec}} = \hat{m}$ .

$\alpha_1$  - for  $\alpha > \alpha_1$  the temperature drops below  $T_{\text{rec}}$  while  $m_{\text{rec}} < \hat{m}$ .

$\bar{t}_2$  - the same as  $\bar{t}_1$  only for the case that  $m_{\text{rec}} < \hat{m}$  (relevant for  $\alpha < \alpha_1$ ).

$\tilde{t}$  - the time when  $T_{\text{rec-in}} = T_{\text{rec}}$ .

**Table A1**

Summary of the analytical description for the step function model. We indicate when the luminosity is affected by recombination and when the temperature drops below the recombination temperature.

8.  $L$ : bolometric luminosity.

9.  $\epsilon$ : energy density.
10.  $\eta$ : thermal coupling coefficient, defined in Eq. (9).
11.  $x_{\text{ion}}$ : ionization fraction.
12.  $T_{\text{cl}}$ : the color temperature.
13.  $T_{\text{rec}}$ : the temperature in which there is a significant change in the ionization fraction due to recombination.
14.  $t_{\text{rec}}$ : the time in which recombination starts in the envelope, this is when the color temperature equals  $T_{\text{rec}}$ .
15. For quantity  $x = m, \rho, r, v$ , the subscripts  $x_{\text{cl}}$ ,  $x_{\text{rec}}$  and the superscript  $\hat{x}$  are for the color shell, recombination shell and luminosity shell respectively.
16. For quantity  $x = \eta, \epsilon, \tau$ , the subscripts  $x_{\text{rec-in}}$  and  $x_{\text{rec-out}}$  are for the internal boundary and external boundary of the recombination shell respectively.
17.  $\kappa_T$ : Thomson opacity.
18.  $t_L$ : the time in which recombination starts to affect the bolometric luminosity.

## REFERENCES

- Arcavi, I., Gal-Yam, A., Cenko, S. B., et al. 2012, ArXiv e-prints
- Arnett, W. D. 1980, ApJ, 237, 541
- Bayless, A. J., Pritchard, T. A., Roming, P. W. A., et al. 2013, ApJ, 764, L13
- Bersten, M. C., Benvenuto, O., & Hamuy, M. 2011, ApJ, 729, 61
- Colgate, S. A. 1974, ApJ, 187, 333
- Dessart, L., Hillier, D. J., Waldman, R., & Livne, E. 2013, MNRAS, 433, 1745
- Falk, S. W. 1978, ApJ, 225, L133
- Grassberg, E. K., Imshennik, V. S., & Nadyozhin, D. K. 1971, Astrophysics and Space Science, 10, 28, 10.1007/BF00654604
- Grassberg, E. K., & Nadyozhin, D. K. 1976, Astrophysics and Space Science, 44, 409, 10.1007/BF00642529
- Imshennik, V. S., Nadezhin, D. K., & Utrobin, V. P. 1981, Ap&SS, 78, 105
- Kasen, D., & Woosley, S. E. 2009, ApJ, 703, 2205
- Klein, R. I., & Chevalier, R. A. 1978, ApJ, 223, L109
- Li, W., Leaman, J., Chornock, R., et al. 2011, MNRAS, 412, 1441
- Litvinova, I. Y., & Nadezhin, D. K. 1985, Soviet Astronomy Letters, 11, 145
- Matzner, C. D., & McKee, C. F. 1999, ApJ, 510, 379
- Maund, J. R., & Smartt, S. J. 2009, Science, 324, 486
- Nakar, E., & Sari, R. 2010, ApJ, 725, 904
- Popov, D. V. 1993, ApJ, 414, 712
- Poznanski, D. 2013, MNRAS, 436, 3224
- Rabinak, I., & Waxman, E. 2011, ApJ, 728, 63
- Seaton, M. J. 2005, MNRAS, 362, L1
- Smartt, S. J., Maund, J. R., Hendry, M. A., et al. 2004, Science, 303, 499
- Utrobin, V. P. 2007, A&A, 461, 233
- Van Dyk, S. D., Li, W., & Filippenko, A. V. 2003, PASP, 115, 1289
- Young, T. R. 2004, ApJ, 617, 1233